Synthesis and Characterization of a New Mebendazole Salt: Mebendazole Hydrochloride

E.V. BRUSAU,[1] G.E. CAMÍ,[1] G.E. NARDA,[1] S. CUFFINI,[2] A.P. AYALA,[3] J. ELLENA[4]

[1]Química Inorgánica, Departamento de Química, Facultad de Química, Bioquímica y Farmacia, Universidad Nacional de San Luis, Chacabuco y Pedernera, 5700 San Luis, Argentina

[2]LRA, ACC-Unidad Ceprocor, Alvarez de Arenales 230, B. Juniors, 5004 Córdoba, Argentina

[3]Departamento de Física, Universidade Federal do Ceará, 60455-900 Fortaleza, CE, Brazil

[4]Instituto de Física de São Carlos, Universidade de São Paulo, Caixa Postal 369, 13560-970 São Carlos, SP, Brazil

Received 19 March 2007; revised 28 June 2007; accepted 12 July 2007

Published online in Wiley InterScience (www.interscience.wiley.com). DOI 10.1002/jps.21164

ABSTRACT: Mebendazole hydrochloride [(5-benzoyl-1H-benzimidazole-2-yl)-carbamic acid methyl ester hydrochloride, MBZ·HCl], a new stable salt of mebendazole (MBZ), has been synthesized and characterized. It can easily be obtained from recrystallization of forms A, B, or C of MBZ in diverse solvents with the addition of hydrochloric acid solution. Crystallographic data reveals that the particular conformation adopted by the carbamic group contributes to the stability of the network. The crystal packing is stabilized by the presence of three N–H...Cl intermolecular interactions that form chains along the *b* axis. The XRD analyses of the three crystalline habits found in the crystallization process (square-based pyramids, pseudohexagonal plates, and prismatic) show equivalent diffraction patterns. The vibrational behavior is consistent with crystal structure. The most important functional groups show shifts to lower or higher frequencies in relation to the MBZ polymorphs. The thermal study on MBZ·HCl indicates that the compound is stable up to 160°C approximately. Decomposition occurs in four steps. In the first step the HCl group is eliminated, and after that the remaining MBZ polymorph A decomposes in three steps, as happens with polymorphs B and C. J Pharm Sci 97:542–552, 2008

Keywords: mebendazole hydrochloride; polymorphism; salt formation; crystal structure; FTIR; Raman spectroscopy; thermal stability

INTRODUCTION

Mebendazole [(5-benzoyl-1H-benzimidazole-2-yl)-carbamic acid methyl ester, MBZ] is a potent, orally active, broad-spectrum anthelmintic used in the treatment of ascariasis, uncinariasis, oxyuriasis, and trichuriasis. MBZ acts by inhibition of glucose uptake in the parasite, resulting in immobilization and death. This drug has been investigated by several authors in relation to polymorphism and physical stability of its solid phases.[1–3] Three polymorphic forms (A, B, and C) displaying significantly different solubilities and therapeutic effects have been identified and characterized.[4,5] Diverse techniques have been applied to identify particular polymorphic forms in samples, infrared spectroscopy being the method of choice whereas X-ray powder

This article contains Supplementary Material available at http://www.interscience.wiley.com/jpages/0022-3549/suppmat.

Correspondence to: G.E. Narda (Telephone: 54-2652-423789x117; Fax: 54-2652-430224;
E-mail: gnarda@unsl.edu.ar)

Journal of Pharmaceutical Sciences, Vol. 97, 542–552 (2008)

diffraction is preferred to quantify polymorphic mixtures 3,6 and references therein].

Complete crystal structure data of MBZ polymorphs is not found in the literature because single crystals seem to be hard to obtain. In spite of this fact, crystal structures of some MBZ solvates determined by single crystal X-ray diffraction have been reported. Mebendazole hydrobromide (MBZ·HBr) was found to crystallize in a monoclinic space group ($P2_1/c$)[7] whereas recrystallization of MBZ in propionic acid (MBZ-propionic acid) yields a 1:1 molecular complex (triclinic, $P\bar{1}$).[8]

MBZ belongs to class II of the biopharmaceutics classification systems (BCS). Several authors pointed out possible differences in the bioavailability of the polymorphs of MBZ.[9,10] Even though some discrepancies are reported in the literature about the relative solubility of forms B and C, all the authors agree that form A is the least soluble one.[1,5,9,11] Thus, form C is pharmaceutically preferred since its solubility is enough to ensure optimal bioavailability without exhibiting the toxicity associated to form B.[5,9,11] Furthermore, a therapeutic trial in 958 school-aged children in Thailand using a placebo and the MBZ polymorphs A and C suggests that form A has similar efficacy than the placebo in controlling hookworms and whipworms infections.[9] Other authors also reported on the polymorph dependence of the anthelmintic efficacy of MBZ and found that at least 30% of the form A in the formulation is enough to suppress the desirable pharmacological activity.[10,12] Taking into account that the polymorph A is the most stable form and therefore the most abundant one, a conversion route of A towards a solid phase with greater solubility needs to be found in order to gain a therapeutic activity level similar to polymorph C.

In the present work we report the salt isolation and characterization of mebendazole hydrochloride (MBZ·HCl), a new stable salt which can easily be obtained from recrystallization of forms A, B, or C in diverse anhydrous organic solvents with the addition of hydrochloric acid solution. Preliminary determinations of powder dissolution in physiological conditions showed the compound to present a dissolution profile similar to that of polymorph C with slightly higher solubility values (to be published). We have focused our interest mainly on the single crystal X-ray diffraction structural analysis and physical characterization by X-ray powder diffraction, Fourier Transform infrared and Raman spectroscopies, and thermal analysis.

EXPERIMENTAL

Materials

All chemicals used were of analytical grade. The polymorphs A and C were provided by the Laboratorio de Control de Calidad de Medicamentos (Universidad Nacional de San Luis, San Luis, Argentina), whereas polymorph B was obtained by recrystallization of polymorph C in acetonitrile (Merck).

Salt Formation

A suspension containing 150 mg of polymorph A (or 100 mg of polymorphs B or C) and 50 mL of absolute ethanol was prepared at 25°C under stirring, then concentrated hydrochloric acid solution (1.4 mL) was added until complete dissolution of the solid. Colorless pseudohexagonal plates (from polymorphs A or B solutions), colorless square-based pyramids or prismatic crystals (from polymorph C solution) suitable for single crystal X-ray analysis were obtained after about 10 days. Colorless square-based pyramids were also obtained by slow dissolution of 5 mg of polymorph A in 50 mL 1 M hydrochloric acid aqueous solution under stirring at room temperature. Crystallization occurs after 2.5 months. The crystalline habits mentioned above were also obtained by recrystallizing MBZ·HCl polycrystalline powder in different pure organic solvents (methanol, acetonitrile, ethyl acetate, chloroform, etc.) and their mixtures.

In addition, all polymorphs yielded polycrystalline MBZ·HCl by dissolution in diverse anhydrous organic solvents such as acetonitrile, methanol and chloroform with the addition of hydrochloric acid solution. The obtained crystalline products were filtered, washed with a hexane–ethanol mixture (20:1) and dried under room conditions for further characterization.

Methods

X-ray diffraction powder diagrams (XRPD) were obtained with a Rigaku D-MAX-IIIC diffractometer using Cu Kα radiation (Ni-filter) and NaCl and quartz as external calibration standards.

Data collection (scans and ω scans with κ offsets) was performed at 293(2) K (up to 55° in 2θ with a redundancy of 4) on an Enraf-Nonius Kappa-CCD diffractometer (95 mm CCD camera on

κ-goniostat) using graphite-monochromated MoKα radiation (0.71073 Å). The program COLLECT[13] was used for the collection of data and the integration and scaling of the reflections, with the HKL Denzo-Scalepack system.[14]

The structure was solved by direct methods with SHELXS-97.[15] The model was refined by full-matrix least squares on F^2 with SHELXL-97.[15] Hydrogen atoms were found in the Fourier difference map, except for ones belonging to the benzene ring which were stereochemically positioned, and further treated with a riding model.[15] The H atoms of the CH and CH_2 groups were set isotropic with a thermal parameter 20% greater than the equivalent isotropic displacement parameter of the atom to which they were bonded; while, for hydrogen of CH_3 and OH groups, the percentage was set to 50%. To prepare materials for publication, SHELXL-97 and ORTEP-3[16] programs were used within WinGX.[17]

Fourier transformed infrared (FT-IR) spectra were recorded on a Nicolet PROTÉGÉ 460 spectrometer provided with a CsI beamsplitter in the 4000–250 cm^{-1} range with 32 scans and spectral resolution of 4 cm^{-1}, using the KBr pellet technique.

FT-Raman spectra were recorded from the original samples on a Bruker IFS55 FT-IR/FT-Raman spectrometer equipped with a Nd:YAG laser (1064 nm excitation line) and a liquid-nitrogen cooled Ge detector. FT-Raman spectra were acquired by accumulating 1024 scans at a spectral resolution of 4 cm^{-1}.

Thermogravimetric (TGA) and differential thermal analysis (DTA) curves were obtained with a Shimadzu TGA-51 Thermal Analyzer and DTA-50 Thermal Analyzer, using platinum pans, flowing air at 50 mL min^{-1} and a heating rate of 10°C min^{-1} from room temperature to 1000°C.

RESULTS AND DISCUSSION

X-Ray Powder Diffraction and Crystalline Habits

As described in the previous section, three crystalline habits, pseudohexagonal plates, square-based pyramids and prismatic crystals (see Fig. 1), were systematically observed depending on the crystallization medium. By comparing the MBZ·HCl PXRD pattern with the ones of the polymorphs of MBZ it was verified that this compound crystallizes in a different structure (Fig. 2). In addition, PXRD patterns and FT-IR spectra of the crystalline habits confirmed that different solvents render the same salt of MBZ.

Crystal Structure

The X-ray analysis revealed that, at the molecular level, MBZ is intimately associated with the hydrochloric acid by complementary hydrogen bonding so that a 1:1 complex unit is formed. The molecular structure and atomic labeling of this unit are shown in Figure 3. Table 1 lists data collection and refinement details. Bond lengths and angles are shown in Table 2.

The comparison of the torsion angles in the MBZ·HCl molecule with the corresponding data for MBZ·HBr and MBZ-propionic acid complex[7,8] shows significant differences in the orientations of the substituents attached to C(2) and C(5) in the unprotonated (MBZ-propionic acid) and in the protonated forms (MBZ·HBr and MBZ·HCl). In all of them, the carbamic group is coplanar with the benzimidazole ring (within experimental error). Nevertheless, different conformations of this group are observed depending on the corresponding compound. These differences in the carbamate group conformations are characterized by rota-

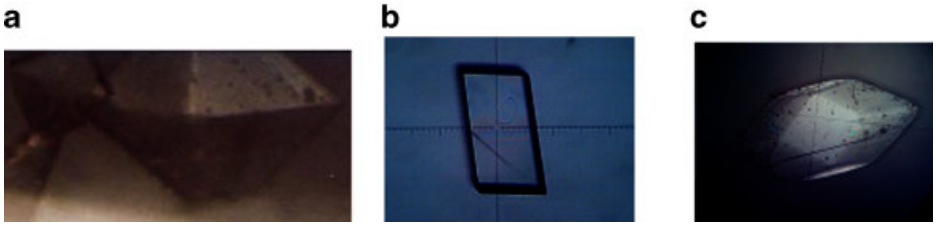

Figure 1. Crystalline habits of MBZ·HCl: (a) Pyramidal square planar habit, (b) Prismatic form and (c) Pseudohexagonal habit.

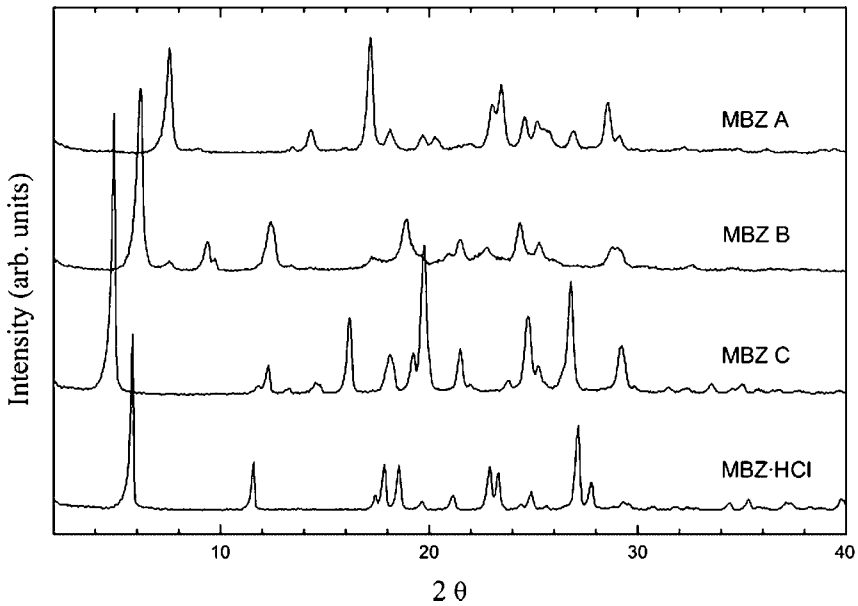

Figure 2. Diffractograms of polymorphs A, B, and C of MBZ compared with MBZ·HCl.

tions around C(2)–N(18) and N(18)–C(19) bonds, as show the following torsion angles values: N(1)-C(2)-N(18)–C(19) 0.000(2)°, −5(3)° and 179.9(4)° of MBZ·HCl, MBZ·HBr and MBZ-propionic acid, respectively], C(2)–N(18)–C(19)–O(20) [180(1)°, 7(3)° and −0.7(7)° of MBZ·HCl, MBZ·HBr and MBZ-propionic acid, respectively], and C(2)–N(18)–C(19)–O(21) [0.000(2)°, 178(2)° and 178.8(3)° of MBZ·HCl, MBZ·HBr and MBZ-propionic acid, respectively]. In this way, the carbamic group of MBZ·HCl presents an intramolecular interaction, $N(3)–H(3)\ldots O(21)_{carbamic}$ (H...O distance: 1.930(3) Å) which would explain the stabilization gained by the cyclic conformation

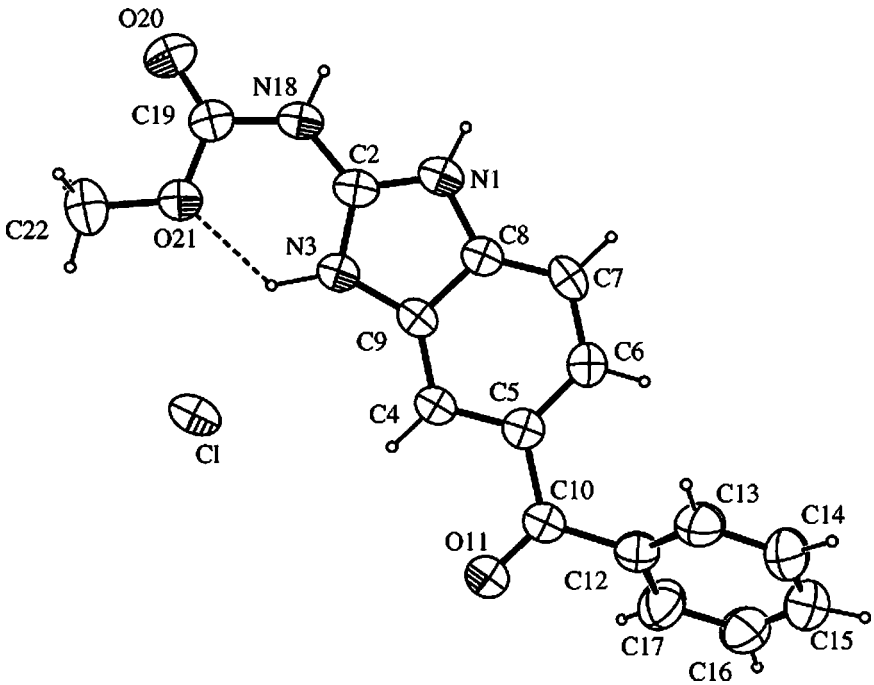

Figure 3. ORTEP view of MBZ·HCl, showing the atoms labeling and the 50% probability ellipsoids.

Table 1. Crystal Data and Structure Refinement

Empirical formula	$C_{16}H_{14}ClN_3O_3$
Formula weight	331.75
Temperature	293(2) K
Wavelength	0.71073 Å
Crystal system	Orthorhombic
Space group	$Cmc2_1$
Unit cell dimensions	$a = 6.5584(6)$ Å
	$b = 7.7934(5)$ Å
	$c = 30.458(2)$ Å
Volume	1556.8(2) Å^3
Z	4
Density (calculated)	1.420 g/cm^3
Absorption coefficient	0.264 mm^{-1}
$F(000)$	692
Crystal size	$0.30 \times 0.22 \times 0.20$ mm^3
Theta range for data collection	4.87–27.5°
Index ranges	$-8 \le h \le 8$, $-10 \le k \le 9$, $-39 \le l \le 39$
Reflections collected	3869
Independent reflections	1836 [R(int) = 0.0604]
Completeness to theta = 27.5°	98.1%
Absorption correction	None
Refinement method	Full-matrix least-squares on F^2
Computing[a]	COLLECT, HKL Denzo and Scalepack SHELXS-97, SHELXL-97
Data/restraints/parameters	1836/1/154
Goodness-of-fit on F^2	1.038
Final R indices [$I > 2\sigma(I)$]	$R_1 = 0.0471$, w$R_2 = 0.1089$
R indices (all data)	$R_1 = 0.0751$, w$R_2 = 0.1224$
Absolute structure parameter	0.0(1)
Largest diff. peak and hole	0.156 and −0.238 e.Å^{-3}

[a]Data collection, data processing, structure solution and structure refinement respectively.

of the carbamate group in MBZ·HCl. This particular interaction is not present in the other structures which in change show intramolecular interactions involving the carbonyl oxygen atom O(20). In the case of MBZ·HBr the interaction is $N(1)_{azolic} - H(1) \cdots O(20)_{carbonyl}$ (H...O distance: 2.199 Å) and in the case of the MBZ-propionic acid is $N(3)_{imine} - H(3) \cdots O(20)_{carbonyl}$ (H...O distance: 2.176 Å).[7,8] These interactions generate a linear structure of the carbamate group.

Concerning the C(5) substituent, it can be seen that the plane containing the benzoyl group and the plane that contains the benzimidazole ring and carbamate group are not coplanar (Fig. 4). In fact, almost all MBZ·HCl molecules are located on a crystallographic mirror plane. Just the benzene ring is out of this plane so that it presents a positional disorder with equal occupation factor. The dihedral angle between molecular mean plane and the aromatic ring is 56.80°. This dihedral angle is 29.4(5)° in MBZ-propionic acid and 63(2)° in MBZ·HBr so that the benzoyl group presents a similar spatial arrangement when occurring in both salts. The same cetonic carbonyl presents a larger rotation and so generates a more perpendicular geometry between the planes. In the case of the co-crystal MBZ-propionic acid, there is a tendency towards a minor rotation of the carbonyl [C(10)–O(11)] generating a more coplanar geometry.

Table 3 presents comparative crystallographic data displaying selected H-bond interactions in MBZ·HCl and MBZ·HBr. The analysis of this table reveals that N(3) is the acceptor of the H from the acid. This fact indicates in MBZ·HCl that azolic-N atom of the benzimidazole is protonated, which is in agreement with the lengthening of the bond distance in $N(3)_{azolic}$–C(2), 1.328(6) Å, similar to $N(1)_{imine}$–C(2), 1.337(5) Å. These values are intermediate between double and single bonds (Tab. 2).[18] In MBZ·HBr, bond distances for $N(1)_{azolic}$–C(2) and $N(3)_{imine}$–C(2) are 1.35(1) Å

Table 2. Selected Bond Lengths [Å] and Angles [°] (with e.s.d.'s in Parenthesis) of MBZ·HCl

O(11)–C(10)	1.217 (5)
O(20)–C(19)	1.191 (6)
O(21)–C(19)	1.323 (5)
O(21)–C(22)	1.442 (6)
N(1)–C(2)	1.337 (5)
N(3)–C(9)	1.408 (5)
N(3)–C(2)	1.328 (6)
N(1)–C(8)	1.399 (6)
N(18)–C(2)	1.359 (6)
N(18)–C(19)	1.372 (5)
C(7)–C(8)	1.375 (6)
C(7)–C(6)	1.375 (6)
C(6)–C(5)	1.403 (6)
C(5)–C(4)	1.404 (6)
C(5)–C(10)	1.485 (6)
C(4)–C(9)	1.385 (6)
C(9)–C(8)	1.393 (6)
C(10)–C(12)	1.501 (7)
C(19)–O(21)–C(22)	115.8 (4)
C(2)–N(3)–C(9)	108.0 (4)
C(2)–N(1)–C(8)	109.0 (3)
C(2)–N(18)–C(19)	129.2 (4)
N(1)–C(2)–N(3)	110.2 (4)
N(1)–C(2)–N(18)	121.2 (4)
N(3)–C(2)–N(18)	128.6 (4)
C(8)–C(7)–C(6)	116.3 (4)
C(7)–C(6)–C(5)	122.9 (4)
C(9)–C(4)–C(5)	116.6 (4)
C(4)–C(9)–N(3)	131.6 (4)
C(8)–C(9)–N(3)	106.7 (4)
C(7)–C(8)–C(9)	122.4 (4)
C(7)–C(8)–N(1)	131.5 (4)
C(9)–C(8)–N(1)	106.1 (4)
O(11)–C(10)–C(12)	118.8 (4)
C(5)–C(10)–C(12)	119.8 (4)
O(20)–C(19)–O(21)	126.3 (4)
O(20)–C(19)–N(18)	122.2 (4)
O(21)–C(19)–N(18)	111.5 (3)

and 1.33(1) Å, respectively,[7] indicating that the interactions present in MBZ·HCl are comparable to those in MBZ·HBr. In the case of MBZ-propionic acid the bond $N(1)_{azolic}$–C(2), 1.314(4) Å, shows a higher double bond character than $N(3)_{imine}$–C(2), 1.348(5) Å.[8]

Figure 4 also shows the intermolecular interactions of MBZ·HCl that stabilize its crystal packing forming chains along the *b* axis. As can be seen from Table 3 both MBZ salts present similar hydrogen bond pattern different form the one in the MBZ-propionic acid which instead form dimers. These interactions lay on the same plane that contains two MBZ molecules (see Tab. 3). Thus, the crystalline structure is stabilized by the formation of planes that contain MBZ molecules interacting with chloride anion in the same direction. Furthermore, these planes are stabilized one on top of the other through Van der Waals interactions between the C(2) atoms and the Cl^- ion on top and below it along the *a* crystallographic axis ($C2\ldots Cl^i = 3.325(5)$ Å; *i*: $1/2+x, y-1/2, z$ and $x-1/2, y-1.2, z$).

Vibrational Spectra

The FT-IR and FT-Raman spectra of MBZ·HCl are presented in Figure 5. Table 4 shows the vibrational modes assignment. Spectra of MBZ·HCl are very rich in bands, so their interpretation is performed on the basis of the most important functional groups present such as carbonyl groups and NH groups in the carbamate and in the benzimidazole ring. The substantial differences between the spectra of MBZ polymorphs A, B, and C and MBZ·HCl rely on these groups.

N–H Modes

In MBZ polymorphs C, A and B, the stretching mode νN–H appears as a single band localized at 3410, 3370 and 3340 cm^{-1}, respectively.[1,11] By comparing these spectra with the ones of benzimidazole[19,20] and carbendazim[21] it is possible to associate these bands with the NH bond belonging to the carbamate moiety, since no intense IR bands of this character are observed in benzimidazole but a similar band is present in carbendazim. On the other hand, MBZ exhibits the broad infrared band around 2900 cm^{-1} characteristic of benzimidazole, whose origin was associated by Klots et al.[19] to tautomeric forms of this compound having also contributions of Fermi resonates.

In the case of MBZ·HCl, no intense bands associated to the νN–H carbamate mode are identified in the IR spectrum around 3300 cm^{-1}, nevertheless the N–H stretching bands are observed at lower frequencies. The first one occurs at 3216 cm^{-1} and is assigned to the imine and carbamate νN–H mode, as their bond distances are equal. The second band appears at 3144 cm^{-1} and is assigned to $N(3)–H_{(HCl)}$ due to its larger N–H bond distance (see Tab. 3). The lowering of the stretching wavenumber associate to the NH bonds is originated in the hydrogen bonds pattern depicted in the previous section. Differently to the polymorphs of MBZ, in the MBZ·HCl, the

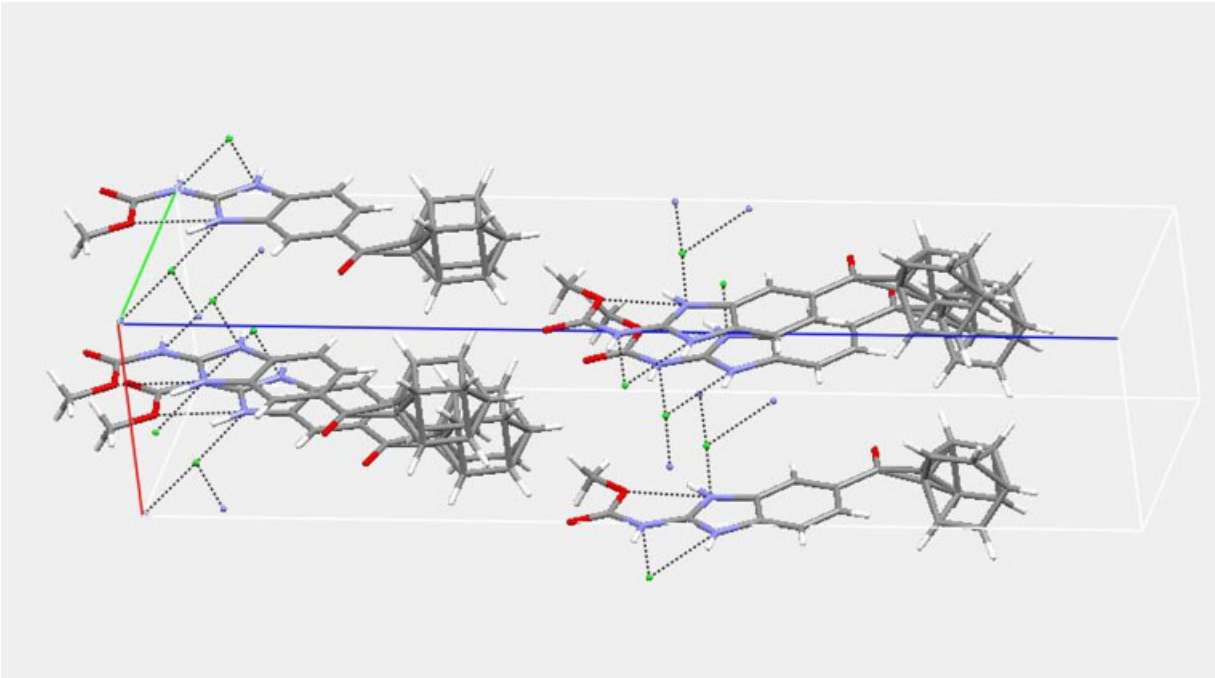

Figure 4. Unit cell of MBZ·HCl.

number of tautomeric forms is reduced due to the hydrogen of the HCl attached to the N(3). However, this effect seems to be not completely suppressed since the characteristic broad band described by Klots et al.[19] is still present.

The imine and carbamate N–H bending modes occur at IR at 1655 and 1634 cm^{-1} while the Raman bands occur at 1655, 1632, 1611, and 1600 cm^{-1}. These modes appear at higher frequencies because the hydrogen bonds in the crystalline structure restrain them from angular bending. Furthermore, the band centered at 1655 cm^{-1} presents two components associated to NH bending and $C{=}O_{cetonic}$ stretching mode.

CO Modes

Polymorphs A, B, and C present $C{=}O_{carbonyl}$ stretching modes at 1730, 1720, and 1700 cm^{-1}, respectively.[1,11] In MBZ·HCl the carbamate C=O bond is reinforced since it is shifted to higher frequencies (1767 cm^{-1} in IR and 1760 cm^{-1} in Raman); as mentioned above, the cetonic carbonyl absorption is assigned at 1655 cm^{-1}.

The performed analysis suggests that in MBZ the carbamic carbonyl group are involved in intra- and/or intermolecular interactions, whereas in MBZ·HCl this functional group does not present these kind of interactions, as it was structurally determined.

Table 3. Selected H-Bonds Data of MBZ·HCl and MBZ·HBr (with e.s.d.'s in Parenthesis)

D-H···A	D–A (Å)	D–H (Å)	D–H–A []
MBZ·HBr			
N(18)-H(18)···Br[a]	3.279 (8)	1.063	144.6 (5)
N(1)-H(1)···Br[a]	3.321 (8)	1.063	141.5 (5)
N(3)-H(3)···Br	3.194 (9)	1.072	144.3 (5)
MBZ·HCl			
N(18)-H(18)···Cl[b]	3.163 (4)	0.860	151.3 (2)
N(1)-H(1)···Cl[b]	3.044 (4)	0.860	146.1 (2)
C(7)-H(7)···O(11)[b]	3.383 (5)	0.930	173.3 (3)
N(3)-H(3)···Cl	3.118 (3)	1.051	131.4 (2)

[a] $x, 1/2-y, 1/2+z$; [b] $x, y+1, z$.

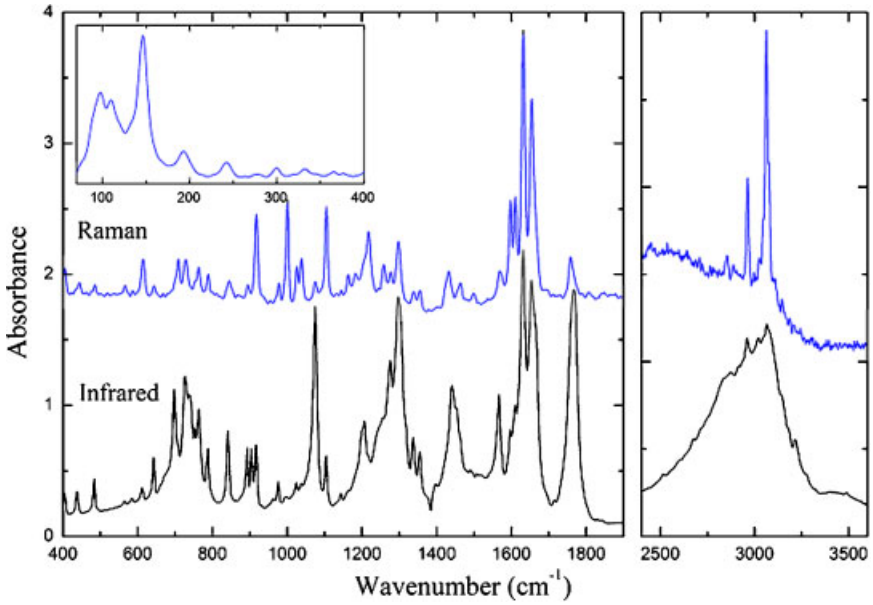

Figure 5. Infrared and Raman (in arbitrary units) spectra of MBZ·HCl.

Concerning the C–O–C mode in MBZ·HCl, one IR band is observed at 1355 cm^{-1}. This band is shifted to lower frequencies than the reference values[22] due to the intramolecular interaction between O(21) and H(1).

C–N Modes

A medium IR intensity band observed at 1567 cm^{-1}, consistent with a low intensity band at 1568 cm^{-1} in the Raman spectrum, is assigned to the νC–N mode. These bands are shifted to lower frequency values than the corresponding to the C=N bond, which agrees with the structural analysis that determines the enlargement of the C–N bond in the benzimidazole ring and the loss of double bond character due to protonation of the azolic nitrogen N(3).

Other C–N stretching mode is overlapped with N–H angular bending at 1634 and 1632 cm^{-1}, in the IR and Raman spectra, respectively. The remaining vibrational modes are showed in Table 4.

Thermal Studies

TGA-DTA curves for MBZ·HCl are shown in Figure 6. Scheme 1 presents the proposed thermal degradation of the compound. The examination of the thermal curves indicates the compound is stable up to ca. 160°C without phase transitions or fusion processes. Decomposition proceeds *via* four stages, the first one being associated to a DTA endothermic signal at 208°C. The experimental weight loss in the TG curve is 10.59% (theoretical, 10.99%) and results are consistent with hydrogen chloride removal yielding polymorph A, the most stable MBZ form, confirmed by IR spectroscopy.

The next mass decay of 13.34% (theoretical, 13.26%) along with the corresponding endothermic peak at 240°C, is related to carbon dioxide elimination. The FT-IR spectrum suggests a type 2 compound (see Scheme 1) as second intermediate produced by an intramolecular rearrangement with the concerted elimination of the gas; this compound is almost identical to that determined by Himmelreich et al.[4] using mass spectrometry when heating MBZ in air up to 270°C.

On further heating, the third mass loss of 12.02% (theoretical: 12.96%) at 335°C (DTA endothermic signal) occurs. The intermediate at this point remains stable up to 651°C, denoted by a strong DTA exothermic signal, where the compound undergoes the last decomposition step with a weight loss of 63.7% (theoretical, 62.79%).

Thermal evolution of the compound resembles to those of the three polymorphic forms of the drug, except for the first stage of decomposition, as is expected. The forms B and C convert to A

Table 4. Selected Vibrational Modes of the Raman and FT-IR Spectra of MBZ·HCl

Mode	Raman—Wavenumbers (cm^{-1})	FTIR—Wavenumbers (cm^{-1})
Modes νNH		
Imidazole		3216 (w)
Amide		3144 (sh)
H-bond		
δNH + νC=O (cetone)	1655 (s)	1655 (s)
δNH + νC–N	1632 (s)	1634 (s)
δNH	1611 (m)	1610 (m)
δNH	1600 (m)	1600 (m)
νCN (benzimidazole)	1568 (w)	1567 (m)
νC=O (carbamate)	1760 (w)	1767 (s)
νC–O–C	—	1355 (w)
νC–C	1297 (m)	1296 (s)
	1259 (w)	1276 (m)
νCH	3063 (s)	3062 (m)
		3022 (w)
	2964 (m)	2960 (m)
		2909 (sh)
		2873 (w)
δCH	1463 (vw)	1455 (sh)
	1431 (w)	1439 (m)
	1218 (m)	1337 (w)
		1142 (vw)
	1105 (m)	1107 (m)
	1076 (vw)	1076 (s)
	1041–1029 (w,d)	1025 (w)
	1000 (m)–979 (vw)	978 (w)
ρCH	919 (m)–846 (vw), 791 (w),	917 (m), 901 (m),
	764 (w), 727 (w), 709 (w)	891 (m) (t)–840 (m)–789 (w)–763 (m),
		738 (sh), 728 (m), 697 (m)–646 (m)
Network modes	613 (w)–407 (w)–244	615 (vw), 584 (vw)–482 (w)–440 (w)–408
	(w)–194 (w)–147 (s)–110, 98 (m,d)	(w)–365 (vw)–279 (m)–247 (m)–231 (w)

s, strong; m, media; w, weak; vw, very weak; sh, shoulder; ν, stretching; δ, deformation; ρ, rocking; wag., wagging; s, symmetric; as, asymmetric.

through a crystalline phase transition around 200°C.[3,4]

CONCLUSIONS

Obtainment, single crystal X-ray diffraction data, spectroscopic and thermal behavior of MBZ·HCl are reported here for the first time. The synthesis of MBZ·HCl is simple and reproducible; the compound can be obtained from any of the three MBZ polymorphs and crystallizes in three different crystalline habits according to the solvent used. Crystallization in the studied solvents does not generate any polymorphic changes in MBZ·HCl. Different conformations of the carbamic group are observed in the case of MBZ·HCl, MBZ-propionic acid and MBZ·HBr.

The vibrational behavior of MBZ·HCl confirms the different interactions determined by structural analysis which strongly affects the functional groups mentioned above. Based on IR-Raman spectroscopy, we have found experimental evidence of different intra- and intermolecular interactions that stabilize the crystalline structure. The observed shifts in the νNH, νCN, and νC=O vibrational modes of MBZ·HCl, compared to those in the three MBZ polymorphs, point out the leading role of chloride ion in the three-dimensional development of the solid. Thus, there are several H-bond interactions between this ion and the different N-H groups, diminishing the

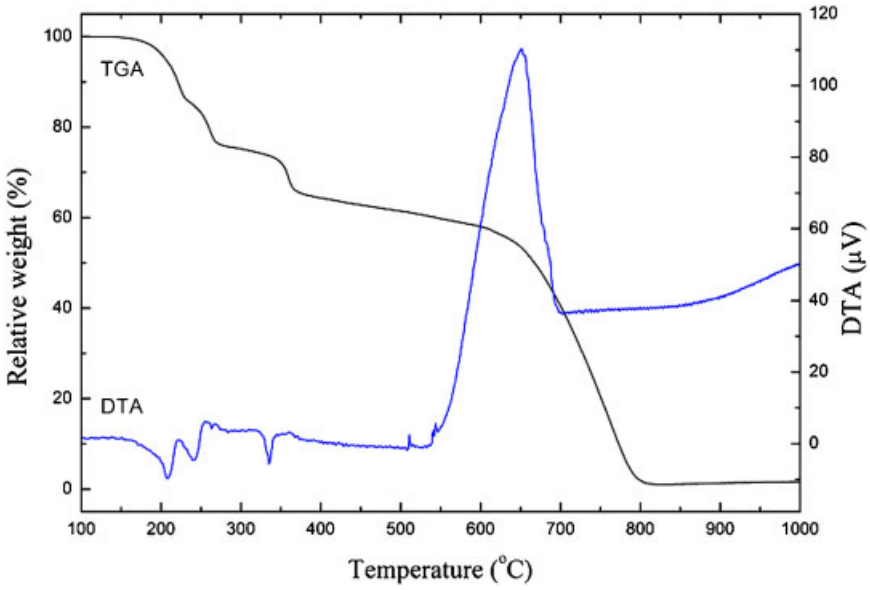

Figure 6. Thermal diagrams of MBZ·HCl.

participation of C=O groups in the H-bond interaction.

MBZ·HCl is stable at temperatures lower than 160°C transforming into MBZ A above this temperature. In the room temperature to decomposition temperature range no solid-solid phase transitions or fusion processes have been observed. On increasing the temperature, the resulting compound follows the well-known decomposition/melting behavior of MBZ.

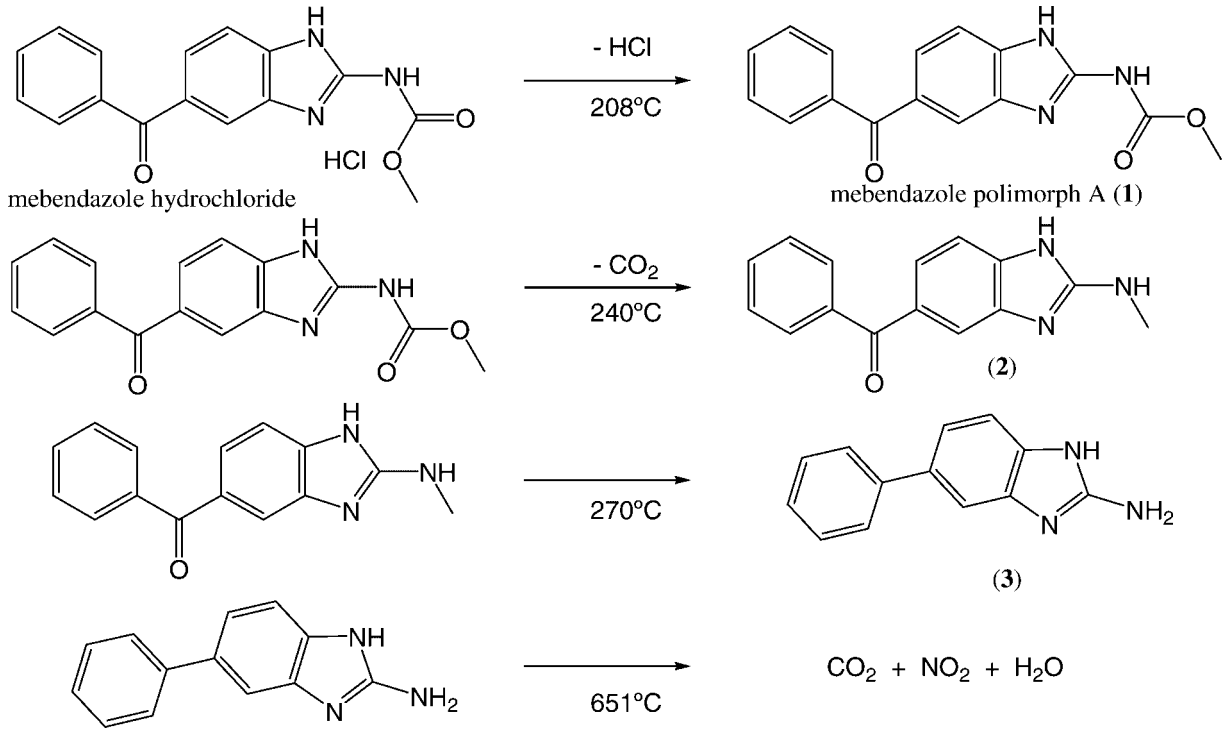

Scheme 1. Proposed thermal degradation of MBZ·HCl.

ACKNOWLEDGMENTS

This work was supported by CONICET, ANPCYT and Universidad Nacional de San Luis. The authors thank to Farm. E. Saidman and Lic. L. Aragón, responsible of the Laboratorio de Control de Calidad de Medicamentos de la Universidad Nacional de San Luis, for supplying the MBZ polymorphs A and C. The authors thank SECyT-UNC and Agencia Córdoba Ciencia of Argentina and CAPES and CNPq of Brazil for financial support. A.P. Ayala acknowledges financial support from the Brazilian Agency CNPq (PDE—Proc. 201246/2004-0) and UNESCO (IBSP Proj. 3-Br-05). G. E. Narda is member of the CONICET.

REFERENCES

1. Swanepoel E, Liebenberg W, de Villiers MM. 2003. Quality evaluation of generic drugs by dissolution test: Changing the USP dissolution medium to distinguish between active and non-active mebendazole polymorphs. Eur J Pharm Biopharm 55:345–349.
2. Swanepoel E, Liebenberg W, Devarakonda B, de Villiers MM. 2003. Developing a discriminating dissolution test for three mebendazole polymorphs based on solubility differences. Pharmazie 58:117–121.
3. de Villiers MM, Terblanche RJ, Liebenberg W, Swanepoel E, Dekker TG, Song M. 2005. Variable-temperature X-ray powder diffraction analysis of the crystal transformation of the pharmaceutically preferred polymorph C of mebendazole. J Pharm Biomed Anal 38:435–441.
4. Himmelreich M, Rawson BJ, Watson TR. 1977. Polymorphic forms of mebendazole. Aust J Pharm Sci 6:123–125.
5. Rodriguez-Caabeiro F, Criado-Fornelio A, Jimenez-Gonzalez A, Guzmán L, Igual A, Pérez A, Pujol M. 1987. Experimental chemotherapy and toxicity in mice of three mebendazole polymorphic forms. Chemotherapy 33:266–271.
6. Aboul-Enein HY, Bunaciu AA, Fleschin S. 2002. Analysis of mebendazole polymorphs by Fourier Transform IR spectrometry using chemometric methods. Biopol Biospectrosc 67:56–60.
7. Blaton NM, Peeters OM, De Ranter CJ. 1980. (5-benzoyl-1H-benzimidazol-2-yl)-carbamic acid methyl ester hydrobromide (Mebendazole. HBr), $C_{16}H_{14}BrN_3O_3$. Cryst Struct Comm 9:181–186.
8. Caira MR, Dekker TG, Liebenberg W. 1998. Structure of a 1:1 complex between the anthelmintic drug mebendazole and propionic acid. J Chem Crystallogr 28:11–15.
9. Charoenlarp P, Waikagul J, Muennoo C, Srinophakun S, Kitayaporn D. 1993. Efficacy of single-dose mebendazole, polymorphic forms A and C, in the treatment of hookworm and Trichuris infections. Southeast Asian J Trop Med Public Health 24:712–716.
10. Evans AC, Fincham JE, Dhansay MA, Liebenberg W. 1999. Anthelmintic efficacy of mebendazole depends on the molecular polymorph. S Afr Med J 89:1118.
11. Costa J, Fresno M, Guzmán L, Igual A, Oliva J, Vidal P, Pérez A, Pujol M. 1991. Polymorphic forms of mebendazole: Analytical aspects and toxicity. Circ Farm 49:415–424.
12. Ren H, Cheng B, Ma J, Hua D. 1987. Yiyao Gongye, 18: 356–359.
13. Enraf-Nonius. 1997–2000. COLLECT. Nonius BV, Delft, The Netherlands.
14. Otwinowski Z, Minor W. 1997. Processing of X-ray diffraction data collected in oscillation mode. HKL Denzo and Scalepack. Methods in Enzymology 276: 307–326. In: Carter CW Jr, Sweet RM, editors. Macromolecular crystallography, part A. New York: Academic Press.
15. Sheldrick GM. 1997. SHELXS-97 and SHELXL-97. Programs for crystal structure resolution and refinement. Germany: University of Göttingen.
16. Farrugia LJ. 1997. ORTEP-3 for Windows—A version of ORTEP-III with a Graphical User Interface (GUI). J Appl Cryst 30:565–566.
17. Farrugia LJ. 1999. WinGX. J Appl Cryst 32:837–838.
18. Allen FH, Kennard O, Watson DJ, Brammer L, Orpen G, Taylor R. 1987. Tables of bond lengths determined by X-ray and neutron diffraction. Part 1. Bond lengths in organic compounds. J Chem Soc Perkin Trans II S1–S19.
19. Klots TD, Devlin P, Collier WB. 1997. Heteroatom derivatives of indene V. Vibrational spectra of benzimidazole 1. Spectrochim Acta A Mol Biomol Spectrosc 53:2445–2456.
20. Morsy MA, Al-Khaldi MA, Suwaiyan A. 2002. Normal vibrational mode analysis and assignment of benzimidazole by ab initio and density functional calculations and polarized infrared and Raman spectroscopy. J Phys Chem A 106:9196–9203.
21. National Institue of Avanced Industrial Science and Technology. SDBSWeb. 2006.
22. Prestch E, Clerc T, Seibl J, Simon W. 1998. Tablas para la dilucidación estructural de compuestos orgánicos por métodos espectroscópicos: 13C-RMN, 1H-RMN, IR, EM, UV-Vis. Barcelona. España: Singer Verlag-Ibérica.